



OPEN

SUBJECT AREAS:

BIODIVERSITY

CORAL REEFS

COMMUNITY ECOLOGY

OCEAN SCIENCES

Environmental variability and biodiversity of megabenthos on the Hebrides Terrace Seamount (Northeast Atlantic)

Lea-Anne Henry¹, Johanne Vad², Helen S. Findlay³, Javier Murillo⁴, Rosanna Milligan⁵
& J. Murray Roberts^{1,6,7}Received
5 March 2014Accepted
16 June 2014Published
7 July 2014Correspondence and
requests for materials
should be addressed to
J.M.R. (j.m.roberts@
hw.ac.uk)

¹Centre for Marine Biodiversity, Heriot-Watt University, Edinburgh, EH14 4AS, United Kingdom, ²École Normale Supérieure de Paris, Département de Biologie, 46 rue d'Ulm, Paris, 75005, France, ³Plymouth Marine Laboratory, Prospect Place, Hoe, Plymouth, PL1 3DH, United Kingdom, ⁴Instituto Español de Oceanografía, Centro Oceanográfico de Vigo, Programa de Pesquerías Lejanas, Apartado 1552, 36390 Vigo, Spain, ⁵Institute of Biodiversity, Graham Kerr Building, University of Glasgow, Glasgow, G12 8QQ, United Kingdom, ⁶Scottish Association for Marine Science, Scottish Marine Institute, Oban, Argyll, PA37 1QA, United Kingdom, ⁷Center for Marine Science, University of North Carolina Wilmington, 601 South College Road, Wilmington, NC 28403-5928, United States of America.

We present the first remotely operated vehicle investigation of megabenthic communities (1004–1695 m water depth) on the Hebrides Terrace Seamount (Northeast Atlantic). Conductivity-temperature-depth casts showed rapid light attenuation below the summit and an oceanographic regime on the flanks consistent with an internal tide, and high short-term variability in water temperature, salinity, light attenuation, aragonite and oxygen down to 1500 m deep. Minor changes in species composition (3–14%) were explained by changes in depth, substratum and oceanographic stability, whereas environmental variability explained substantially more variation in species richness (40–56%). Two peaks in species richness occurred, the first at 1300–1400 m where cooler Wyville Thomson Overflow Water (WTOW) mixes with subtropical gyre waters and the second at 1500–1600 m where WTOW mixes with subpolar mode waters. Our results suggest that internal tides, substrate heterogeneity and oceanographic interfaces may enhance biological diversity on this and adjacent seamounts in the Rockall Trough.

The ecology of seamount communities in the deep sea is governed by multiple drivers including environmental heterogeneity, intrinsic community dynamics (migration, extinction, species interactions^{1,2}), and disturbance (fishing) history³, the importance of which varies between seamounts. The presence of internal tides, heterogeneity in seabed substrata, and temperature changes often vary with depth on a single seamount, creating substantial changes in species turnover^{4,5} and genetic variability⁶ even on the same seamount.

Although such general trends in the ecology of seamount communities in the deep sea are emerging, continued seamount exploration and monitoring have global importance in an era of expanding human activities penetrating deeper into the oceans. Despite a long history of scientific exploration in areas such as the Rockall Trough in the northeast Atlantic⁷, only 0.4–4.0% of global seamounts have been explored with scientific purpose⁸. For example, biological communities on only two of the three seamounts in the Rockall Trough (Rosemary Bank and Anton Dohrn Seamounts) have actually been surveyed. This hinders our understanding of how these seamounts contribute to the wider structure and function of deep-sea ecosystems in the northeast Atlantic⁸. Unexplored seamounts are also at risk of having an under-developed evidence base to underpin their protection because the biological or ecological value of these seamounts, necessary for conservation prioritisation⁹, cannot be ascertained.

Today, dropframe camera and remotely operated vehicle (ROV) technologies can provide contiguous and geo-referenced replicates of high-resolution imagery ideally suited to seamount exploration and examining paradigms of seamount ecology across space and time in the deep sea. Dropframe camera surveys of the Anton Dohrn and Rosemary Bank Seamounts in the Rockall Trough have revealed a range of habitats including cold-water corals reefs, coral gardens, and dense aggregations of habitat-forming sponges and xenophyophores^{10–13}, but these also



showed evidence of fisheries impacts¹⁴. Benthic communities on the third seamount in the Rockall Trough, The Hebrides Terrace Seamount (HTS; Figure 1), were only recently surveyed using a camera-equipped ROV combined with oceanographic profiling¹⁵. The HTS is an elliptical flat-topped guyot formed in the early Cenozoic during three phases of volcanic activity beginning 62 Myr after the mass extinction event at the end of the Cretaceous¹⁶. The HTS is surrounded by Plio-Pleistocene debris deposits up to 900 m thick, but is also marked by evidence of more recent seismic events along its southern edge¹⁷. Numerous canyons, gullies and escarpments occur along the southern and western flanks of the seamount¹⁸. It rises from depths of around 2300 m to 1000 m deep¹⁹, several hundred metres deeper than the summits of the other seamounts in the Rockall Trough.

The HTS was already known to be important for both marine cetaceans and fish, with recent sightings of fin whale *Balaenoptera physalus*, long-finned pilot whale *Globicephela melas*, harbour porpoise *Phocoena phocoena* and beaked whale, likely *Mesoplodon bidens*²⁰. Large spawning aggregations of orange roughy (*Hoplostethus atlanticus*) on the HTS were discovered in the early 1990s but these were rapidly overexploited within a decade and the fishery has since been abandoned^{21,22}. Dense occurrences of cold-water corals and sponges at the other two seamounts, combined with occurrences of marine cetaceans, fish spawning aggregations, and possibly an isolated stock of *H. atlanticus* on the HTS, suggest that oceanographically dynamic conditions at this seamount²³ may help concentrate high quality food sources for both visiting and resident seamount fauna²⁴, a functional role that should also support biologically rich seamount communities.

The oceanographic setting of the Rockall Trough bathing its seamounts is also both spatially and temporally dynamic^{25,26}, with the interface between water masses being important zones of biotic change^{7,27}. Surface waters (SW) are derived from the westward-flowing North Atlantic Current (NAC) and overlay an upper layer centred around 600–1200 m of northward-flowing warm saline Eastern North Atlantic Water (ENAW) that forms in the Bay of Biscay. In the vicinity of the HTS, ENAW is often mixed with mid-depth outflow of Mediterranean Water (MW) and Sub-Arctic Intermediate Water (SAIW) the latter which derives from the western boundary current of the subpolar gyre, a mixture that varies annually²⁶. Below 1200 m, cooler dense overflow waters are derived from the Norwegian Seas that flow through the Faroese Channels and over the Wyville Thomson Ridge²⁸. This Wyville Thomson Ridge Overflow Water (WTOW) is recorded as far south as 55°N in the Rockall Trough and is itself mixed with MW and SAIW,

although WTOW signals >1500 m water depth are likely attributed to large periodic overflow events²⁸. Beginning around 1500–1600 m, WTOW transitions to Labrador Seawater (LSW) down to about 2000 m water depth²⁶. Cool, fresh LSW is formed by deep winter convective mixing in the Labrador Basin and exported eastwards by the subpolar gyre into the southern entrance of the Rockall Trough²⁹.

Thus, the objective of our study was to use the ROV images and oceanographic profiles to investigate environmental variability, species richness and megabenthic species composition across the HTS.

Results

Oceanographic and hydrographic variability at the HTS. ROV-based conductivity-temperature-depth (CTD) measurements showed that the HTS is bathed by several water masses (Figures 2 and 3, Tables 1 and 2). The summit at (~1000 m water depth) is mostly covered by ENAW, but between 800–1000 m there are distinct waves of high salinity MW. ENAW extends to about 1200 m, where mixing with WTOW and SAIW occurs. The transition from ENAW to WTOW at about 1200 m overlaps with high variability in the particle attenuation coefficient (C_p), salinity and temperature (Figures 2 and 3, Table 2) that persists until about 1500 m. Between 1200–1600 m the waters were mostly WTOW, which is cooler and fresher, less dense and with higher dissolved oxygen (DO) concentrations than ENAW (Figures 2 and 3). Deeper than 1500 m, there is less variation in temperature, salinity and DO (Table 2) and thus we term this layer as oceanographically more “stable” than the “dynamic” layer above 1500 m water depth. Near the end of the dive transects at depths ≥ 1600 m there was increasing penetration of LSW characterised by even higher DO (>260 $\mu\text{mol/L}$) than WTOW (Figures 2 and 3; Table 2).

DO, dissolved inorganic carbon (DIC), C_p , total alkalinity (TA), aragonite saturation state (Ω) and pH all varied with depth (Figure 2, Table 2). Steep declines in the concentration of oxygen occurred at 800–1000 m water depth with an oxygen minimum of 203 $\mu\text{mol L}^{-1}$ at 1000 m water depth, after which DO steadily increased up to 256 $\mu\text{mol L}^{-1}$ at 1930 m water depth. Oxygen saturation was nearly 100% at the surface, decreased to about 68% near 1000 m and increased below 1000 m back up to about 77% at 1930 m (Table 2).

The seamount summit experienced little change in C_p , ranging between 0.15–0.16 m^{-1} (Figure 2). Thereafter sustained high variability in C_p ranging between 0.1–0.2 m^{-1} persisted down to 1500 m water depth (Figure 2, Table 2).

Aragonite saturation decreased from 1.33–1.38 at the seamount summit to as low as 1.11 at a depth of 1930 m (Figure 2, Table 2). Estimated $\Omega_{\text{aragonite}}$ for the ROV transects revealed saturation states

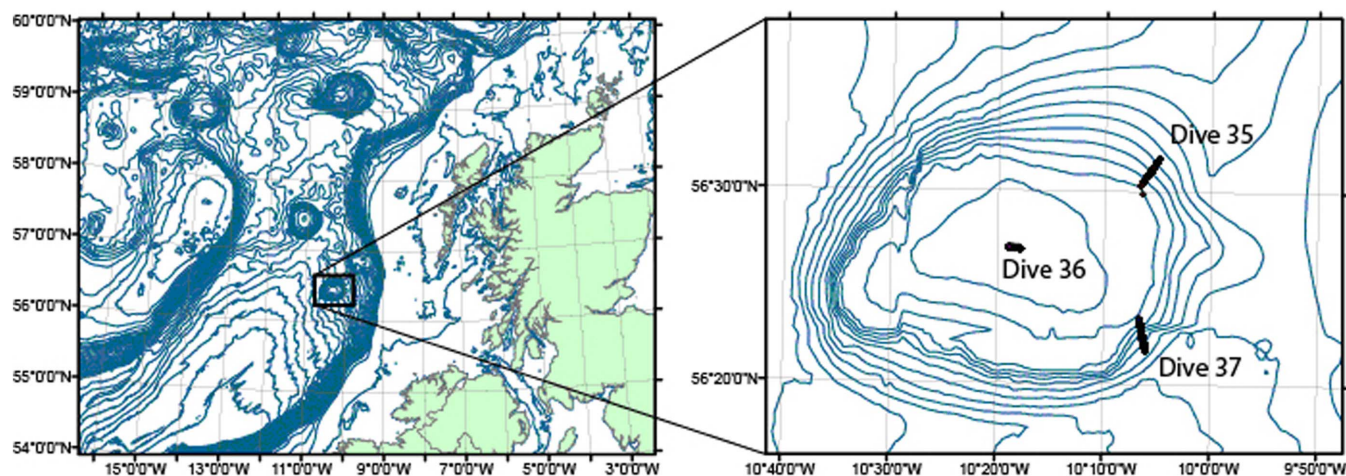


Figure 1 | Location of the Hebrides Terrace Seamount in the southcentral Rockall Trough and the three ROV dive transects on the seamount summit and flanks (inset). Maps were generated using ArcGIS version 9.3.

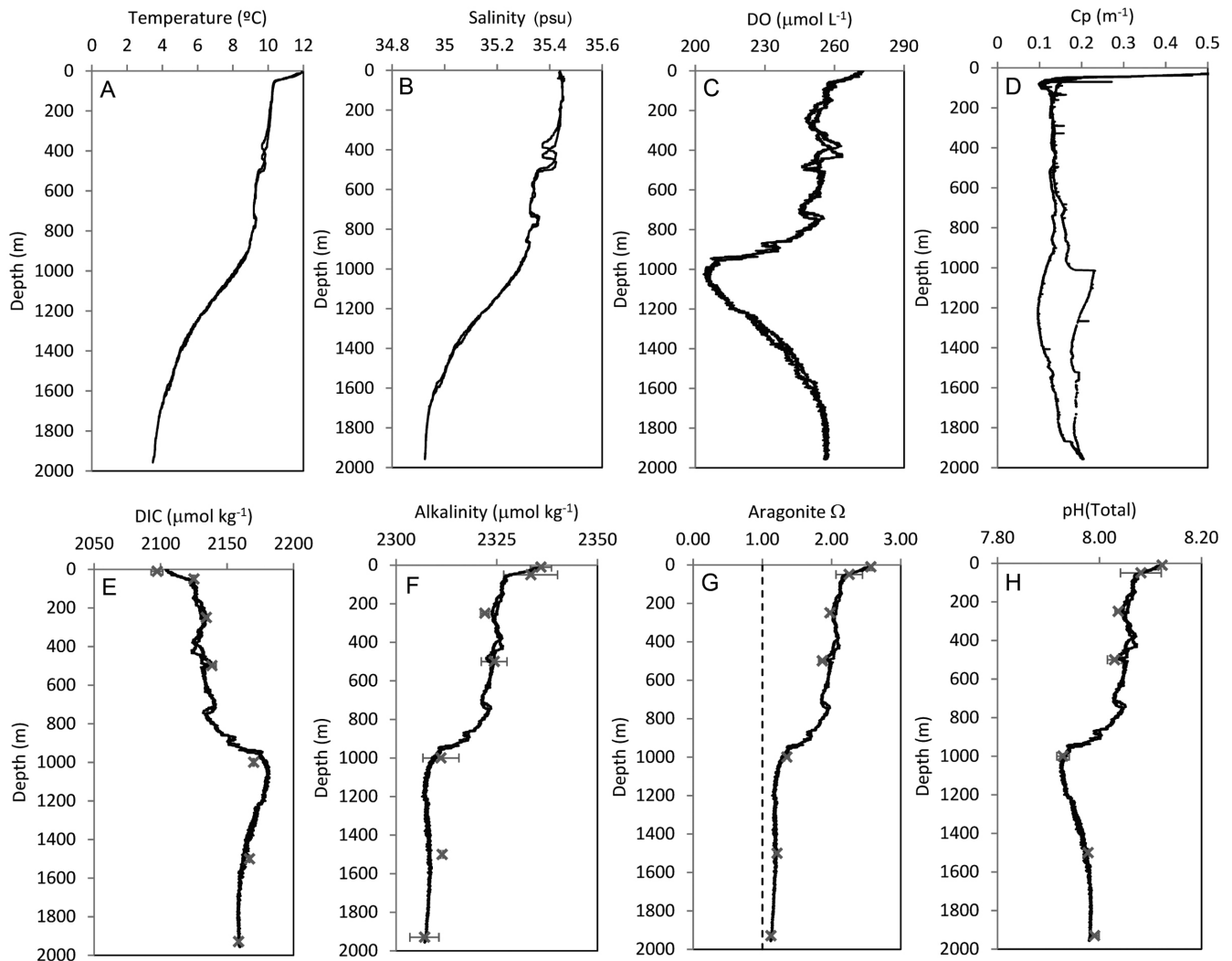


Figure 2 | Depth profiles from the full CTD cast (0–1930 m water depth), showing measured (A): temperature ($^{\circ}\text{C}$), (B): salinity (psu), (C): dissolved oxygen concentration (DO), (D): particle attenuation coefficient (C_p), (E): dissolved inorganic carbon (DIC), (F): total alkalinity (TA), and calculated (G): aragonite saturation state, and (H): pH (total scale). In figures (E–H) black crosses indicate the mean value of the data collected from water samples (error bars are 1 standard deviation).

< 1 on several occasions, reaching as low as 0.76. $\Omega_{\text{aragonite}} > 1$ is a state when thermodynamically, aragonite mineral precipitation occurs, whereas $\Omega < 1$ is a state when thermodynamically aragonite dissolves. Thus our CTD measurements indicate a degree of periodic undersaturation on the deep seamount flanks.

Natural history. A total of 109 megafaunal taxa were identified (Supplementary Table S1). The giant agglutinated xenophyophore *Syringammia fragilissima* was the most frequently observed species, present in 66% of images. Elasmobranch egg cases from at least two species were observed at 16 stations on the flanks in waters 1523–1651 m deep; some were observed among coral branches of the reef-framework-forming scleractinian *Solenosmilia variabilis*, similar to the way in which shark egg capsules are observed on cold-water coral reefs formed by another scleractinian, *Lophelia pertusa*³⁰. Their identities have not yet been confirmed with archived museum collections so these egg cases were not included in the benthic analyses. One sponge species identified tentatively as ?*Halichondria (Eumastia) sitiens* from dive 037 is known to contain bioactive anti-cancer compounds³¹.

A total of 26 taxa were tentatively identified to species level, all of which have broad North Atlantic or global ranges. All four fish taxa identified to species level are distributed across the North Atlantic including the oreostomatid *Neocyttus helgae* that frequently

co-occurs with seamount cold-water corals and sponges³². Many had Lusitanian or Arctic affinities that suggest the HTS is inhabited by a rich mixture of faunae from the north and south via the different water masses that bathe this seamount. We caution however that because our species identifications were based solely on ROV images, some species could actually represent cryptic species. Morphological and molecular data as presented in Cárdenas *et al.*³³ for the geodiid species in the Atlantic boreo-arctic region will be needed to validate our identifications.

Species richness. In contrast to low species numbers on the summit (dive 036, mean number of species per transect = 4.5, s.e.m. = 0.1), the seamount flanks (dives 035 and 037) were densely colonised by species-rich assemblages (mean = 8.7, s.e.m. = 0.3 and mean = 7.1, s.e.m. = 0.2, respectively) including habitat-forming fauna such as *Syringammia fragilissima*, geodiid sponges and the reef framework-forming scleractinian coral *Solenosmilia variabilis*. Megafauna inhabiting *Solenosmilia* framework on the HTS were similar to those living among *Lophelia* framework on nearby banks and seamounts e.g. black corals of the genus *Stichopathes*, glass sponges, encrusting sponges, ophiuroids and crinoids^{11,34–36}.

Although there was a lot of variability in the number of species from image to image, richness on the flanks appeared to begin

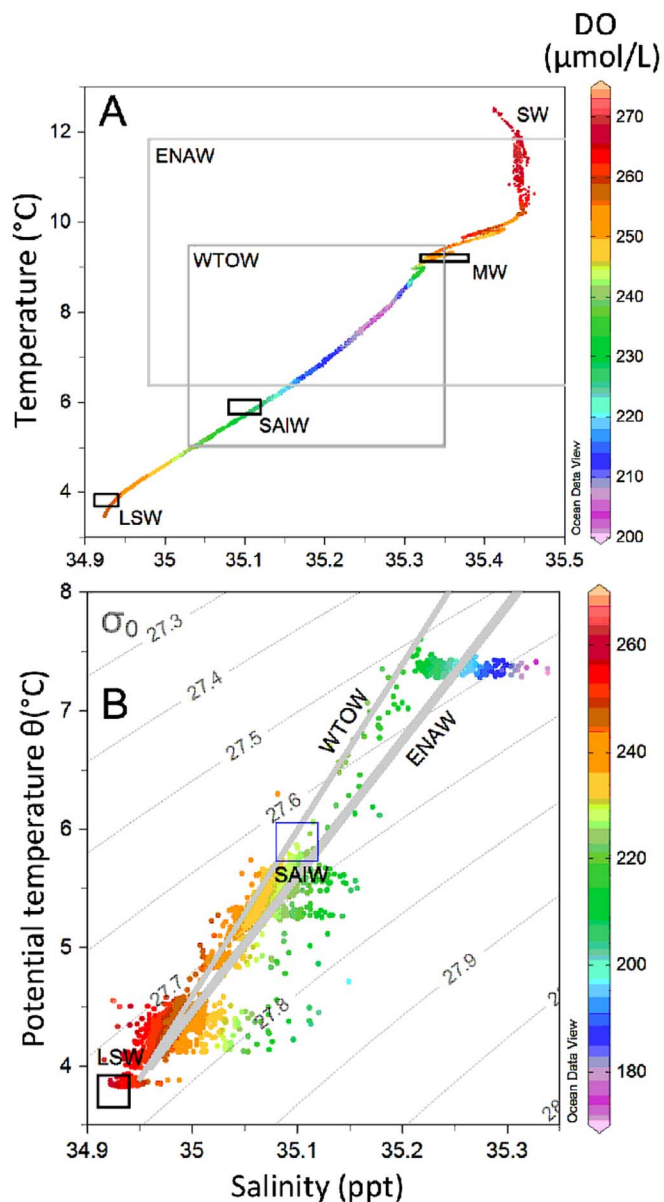


Figure 3 | Water mass properties at the HTS. (A): T-S and DO conditions encountered on the HTS through a vertical profile from the surface to 1930 m. (B): T-S and DO conditions for the ROV dives 035, 036 and 037 with density (σ) contours. Water mass indicators for SW, (surface waters), ENAW (Eastern North Atlantic Water), WTOW (Wyville Thomson Ridge Overflow Water), MW (Mediterranean Waters), SAIW (Sub-Arctic Intermediate Water) and LSW (Labrador Seawater) properties are shown as either boxes or mixing-lines. Representative values for water masses were taken from McGrath *et al.*²⁶ for the Rockall Trough.

increasing at around 1250 m water depth, peaking around 1300–1400 m, then decreasing again (Figure 4). A second peak in richness seemed to occur around 1500–1600 m (Figure 4). Non-parametric regression of species richness on the flanks showed that a substantial proportion of variation in the number of species (between 40–56%) was explained by depth, substratum, water mass identity, and interactions between them (goodness of fit $R^2_{\text{dive035}} = 0.55$, $R^2_{\text{dive037}} = 0.40$). Little variation in richness on the summit was explained by this combination of variables (goodness of fit $R^2_{\text{dive036}} = 0.02$).

Changes in species composition. Substrata and oceanography did not vary at the summit as they did on the flanks, the latter which exhibited significant changes in species composition related to

stronger downslope environmental gradients (Figure 5). Strong community dissimilarity was detected from an analysis of similarities (ANOSIM) between communities on the summit and the flanks, with habitat-forming sponges, corals and xenophyophores down the flanks but which were virtually absent on the summit.

Community dissimilarity on the northeast flank (dive 035) was strongly related to downslope shifts in the predominant substrata, which changed from coarse sand to gravels, cobble, bedrock and coral framework (Supplementary Table S2; Figure 5). Communities significantly (ANOSIM global $R = 0.32$, $p = 0.001$) differed across most substrata except for cobble and very coarse gravel, and cobble and bedrock, each of which could not be significantly discriminated ($p = 0.40$ and 0.89 , respectively; Supplementary Table S2). With increasing depth, similarity of percentages (SIMPER) analyses revealed how assemblages changed from one dominated mostly by sponges such as *Periphragella lusitanica*, *Hamacantha* sp. and *Hexadella dedritifera* on very coarse gravel, to *S. fragilissima*, sponges and ophiuroids on cobble, then to one characterised by sponges, ophiuroids and the antipatharian coral *Stichopathes cf abyssicola* on bedrock, and coral framework characterised by *Solenosmilia variabilis*, sponges and ophiuroids (Supplementary Table S2).

Community dissimilarity on this flank was also strongly related to differences in oceanographic variability (ANOSIM Global $R = 0.17$, $p = 0.001$; Supplementary Table S2). SIMPER detected differences between assemblages bathed by more dynamic versus stable waters including more occurrences of sponges, antipatharians, solitary corals, and the reef-building coral *S. variabilis* at depths > 1500 m and more *Syringammina fragilissima* at oceanographically more dynamic stations (Supplementary Table S2).

Community dissimilarity on the seamount's southeastern flank (dive 037) was also related to downslope changes in substrata but not as strongly as for dive 035 (ANOSIM Global $R = 0.15$, $p = 0.001$; Supplementary Table S2). Shallow stations began on coarse gravel facies and changed to patches of cobble, bedrock, and coral framework then finally to fine sands at the deepest stations (Figure 5; Supplementary Table S2). Communities that did significantly differ were characterised by SIMPER as being comprised of sponges, *Stichopathes cf abyssicola* and *Solenosmilia variabilis* on coarser grained substrata to those with higher occurrences of *Syringammina fragilissima* on finer grained sands (Supplementary Table S2).

Community dissimilarity on dive 037 was also related to downslope shifts in oceanographic variability (ANOSIM Global $R = 0.14$, $p = 0.001$; Supplementary Table S2). Differences identified by SIMPER were driven primarily by higher proportions of *Stichopathes cf abyssicola* and ophiuroids at deeper more stable stations while the large glass sponge *Periphragella lusitanica* occurred more frequently at oceanographically dynamic settings <1500 m deep (Supplementary Table S2).

Although community dissimilarity was closely related to environmental variability, in fact only a modest amount of change in species composition could be directly explained by gradients in these variables or by the effects of geographic distance between stations. In total, environmental and geographic distance explained statistically significant ($p < 0.01$) amounts of change in species composition on the seamount flanks (12–14% in dives 035 and 037, respectively) and on the summit (3% in dive 036; Supplementary Table S3). The change in substrata and oceanography during dives 035 and 037 detected during the SIMPER analyses were again reinforced in the species-environment biplots as were the species associations including habitat-forming corals characterising deeper stations (Figure 6).

Discussion

Our study established for the first time the high benthic biological diversity and occurrences of habitat-forming megafauna on the HTS alongside an oceanographically and hydrographically dynamic setting. Changes in species composition were related to differences



Table 1 | ROV transects on the Hebrides Terrace Seamount together with ROV CTD range for temperature, salinity, and estimated oxygen % and estimated aragonite saturation state

	Dive 035	Dive 036	Dive 037
Date of dive (dd/mm/yyyy)	09/06/2012	10/06/2012	10/06/2012
Transect length	3157 m	1040 m	2972 m
Subset # of images analysed	319	84	292
Subset duration (hours:minutes:seconds)	06:56:30	01:42:57	06:26:24
Geomorphology	flank	summit	flank
Depth range	1238–1695 m	1004–1021 m	1234–1661 m
Temperature range	4.56–6.40	7.50–7.62	3.97–5.43
Salinity range	34.97–35.17	35.22–35.24	34.95–35.09
Oxygen saturation (%)	63.6–83.8	58.3–74.3	62.3–82.0
Aragonite saturation state	0.77–1.40	0.87–1.36	0.77–1.35
Total # observed megafauna species	80	33	56

between the summit and flank, which differed in the presence of an internal tide impinging on the sloping flanks of the seamount at 1200–1600 m water depth. Oceanographic variability and changes in substratum were related to changes in species composition on the flanks, but neither variable directly explained many of these changes. In contrast, between 40–56% of changes in species richness was explained by this environmental variability. Notably, two peaks in species richness centered at the interface between different water masses suggest a critical role of oceanographic variability in enhancing richness. Thus our findings reinforce the notion that seamount fauna do respond to environmental variability across different spatial scales, e.g. summit versus flank or downslope, but in species-specific ways³⁷ and in such a way that they cannot be directly explained using categorical variables such as water mass, or predominant substratum.

Community dissimilarity between the seamount summit and flanks was likely related to seamount-generated flow variability such as internal tides and mixing^{1,38}. Critically, internal tides and enhanced mixing bring food particles to deep-sea benthos that increases community similarity across wide areas over which these features occur³⁹. Hydrographic variability creates community dissimilarity on the Great Meteor Seamount off the Azores⁴⁰, and our evidence also supports this notion for the HTS where long sections of the flanks were inhabited by large habitat-forming sessile suspension-feeding corals and sponges. We note that very little evidence of fishing disturbance was evident during the dive on the summit: thus it is more likely that community dissimilarity between the summit and flanks were likely due to the presence of hydrographic features such as an internal tide.

Surface currents are enhanced and strongly baroclinic over the HTS⁴¹, the abrupt topography of which generates an internal tide^{41,42} that is strongly displaced in two zones centered on the 600 m and 1200–1600 m water depth contours⁴³. Given the high density and diversity of large suspension-feeding fauna strictly on the flanks, our biological and CTD data support the notion of this internal tide delivers higher concentrations of particles to the seamount flanks (Figures 2, 3) than at the summit, which in turns substantially alters

species composition between summit and flanks. Benthic megafauna on the adjacent Anton Dohrn Seamount are remarkably similar to those documented here, with enhanced densities of habitat-forming sponges, corals and xenophyophores at comparable depths^{13,44}. Notably, there is also a strong internal tide that propagates from Anton Dohrn⁴¹, which likely plays an equivalent role on this seamount as it does on the HTS.

Community dissimilarity was also detected between oceanographically dynamic versus more stable water mass layers. Our CTD measurements documented oceanographic transitions from warmer more saline ENAW to deeper layers of WTOW and then to cooler and fresher LSW. This transition structures benthos across the wider Rockall Trough^{7,27} as similar interfaces do for seamount taxa globally^{4,45}. Of particular note at the HTS were the relatively higher frequency of *Solenosmilia variabilis* at depths with more short-term thermohaline and oxyc stability, and more frequent occurrences of the large xenophyophore *Syringammina fragilissima* at shallower stations that had higher short-term oceanographic variability.

Some of the species-specific responses to downslope changes on the HTS can be attributed to changes in chemical oceanography. For example, the oceanographic setting at depths beyond 1500 m water depth is ideally suited to the environmental niche of *S. variabilis*. This species can inhabit cooler less saline waters that are less saturated in aragonite and higher in oxygen⁴⁶ than another ubiquitous reef-forming coral in the Rockall Trough, *Lophelia pertusa*, which tends to inhabit seamounts < 1200 m water depth in the Rockall Trough⁴⁴. Other variables such as DIC, alkalinity, pH and potential water mass density constrain the distribution of *L. pertusa*⁴⁷, however effects on occurrences of *S. variabilis* are not unknown. Depth is known to be a strong predictor of suitable habitat for *S. variabilis* as is the presence of a seamount^{46,48}. Given that *S. variabilis* also exists along restricted salinity and temperature ranges⁴⁶, our study suggests that the relationship with increasing depth on seamounts is perhaps better explained by oceanographic stability and geochemical constraints such as oxygen concentration, which may also be depth-related.

Table 2 | Means and ranges of oceanographic variables on the HTS recorded by the full CTD cast. Ranges of salinity, temperature, particle attenuation coefficient (C_p), oxygen and aragonite saturation states were two to three times higher at stations 1200–1500 m (the oceanographically “dynamic” layer) throughout most of the WTOW layer than at (oceanographically stable) > 1500 m water depth

	Salinity (psu)	Temperature (°C)	C_p (m^{-1})	O ₂ saturation (%)	Aragonite saturation
Means					
1200–1500 m	35.07	5.38	0.14	74.56	1.18
1500–1700 m	34.97	4.27	0.16	77.80	1.18
Ranges (max-min)					
1200–1500 m	0.08	0.93	0.06	3.63	0.04
1500–1700 m	0.03	0.40	0.03	1.35	0.03

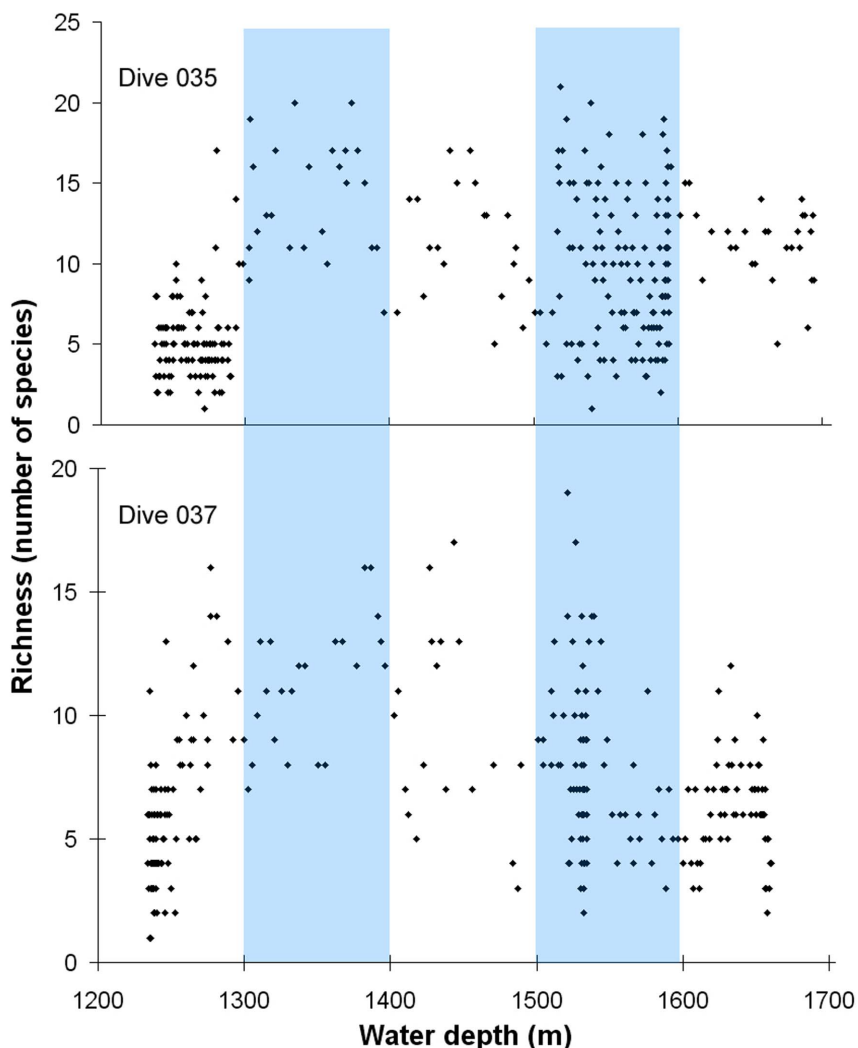


Figure 4 | Depth-related trends in species richness per image during dives 035 and 037. Blue bars indicate what appear to be peaks in species richness.

On the continental slope to the west of Britain, the agglutinated xenophyophore *Syringammina fragilissima* is typically encountered in depositional environments characterised by enhanced surface production and particle flux⁴⁹. Thus enhanced frequencies of this species at oceanographically variable stations on the flanks of the HTS are probably explained by the greater range of C_p values recorded by CTD at depths 1000–1500 m which would supply more particles to these stations.

Substratum heterogeneity significantly altered species composition on the flanks of the HTS as it does on other seamounts^{1,4}. Occurrences of deep-sea reef framework-forming corals in particular alter species composition and effectively triple species richness⁵⁰. Coral reef framework on the HTS was formed by *Solenosmilia variabilis*, and comprised a very rich mixture of associated species including black corals, bamboo corals, cup corals, sponges, crinoids and tunicates, all of which further enhance diversity themselves by providing more habitats.

We documented two peaks in the number of megafaunal taxa on the HTS, the first of which corresponds to previous studies. The interface between warm and cool layers in the Rockall Trough at around 1100 m water depth are known to increase benthic abundance and diversity⁷, both of which peak around 1400 m water depth²⁷. Likewise, richness on the HTS peaked at 1300–1400 m water depth, but we also uncovered an additional distinct peak between 1500–1600 m water depth. Our CTD data showed transitions from WTOW to LSW at these depths, which could foster the rich mixture

of fauna we observed, some with cool Arctic or warmer Lusitanian biogeographic affinities.

Our ROV and CTD investigations captured a snapshot of the total environmental and biological variability on the HTS. Over the last two decades, upper and lower layer water mass pH in the Rockall Trough has dropped along with the aragonite saturation state²⁵ while levels of DIC have increased, all of which challenge the ability of deep-sea species such as cold-water corals to adapt or acclimate⁴⁷. The discovery of periodic aragonite undersaturation on the deep flanks of the HTS likely has implications for ecosystem functioning as well. Organisms with aragonitic calcium carbonate skeletons such as *S. variabilis* are at risk from dissolution and must either be physiologically pre-adapted to these conditions or struggle to produce their skeletons.

Combined with the rapid pace of climate change²⁵, deep-sea habitats in the Rockall Trough are now marked by the footprint of commercial bottom fisheries, an activity with an impact at least an order of magnitude greater than all other human activities in the northeast Atlantic⁵¹. Although we documented 16 sites with elasmobranch egg cases, densities of sharks and other fish such as orange roughy on the HTS have declined 40-fold since the 1970s⁵² and suggest that any such spawning grounds should be urgently prioritised as deep-sea conservation features. No orange roughy were recorded during our survey, the intensive fishery for this species having declined long before scientific investigation of this seamount began, as is often the case⁵³.

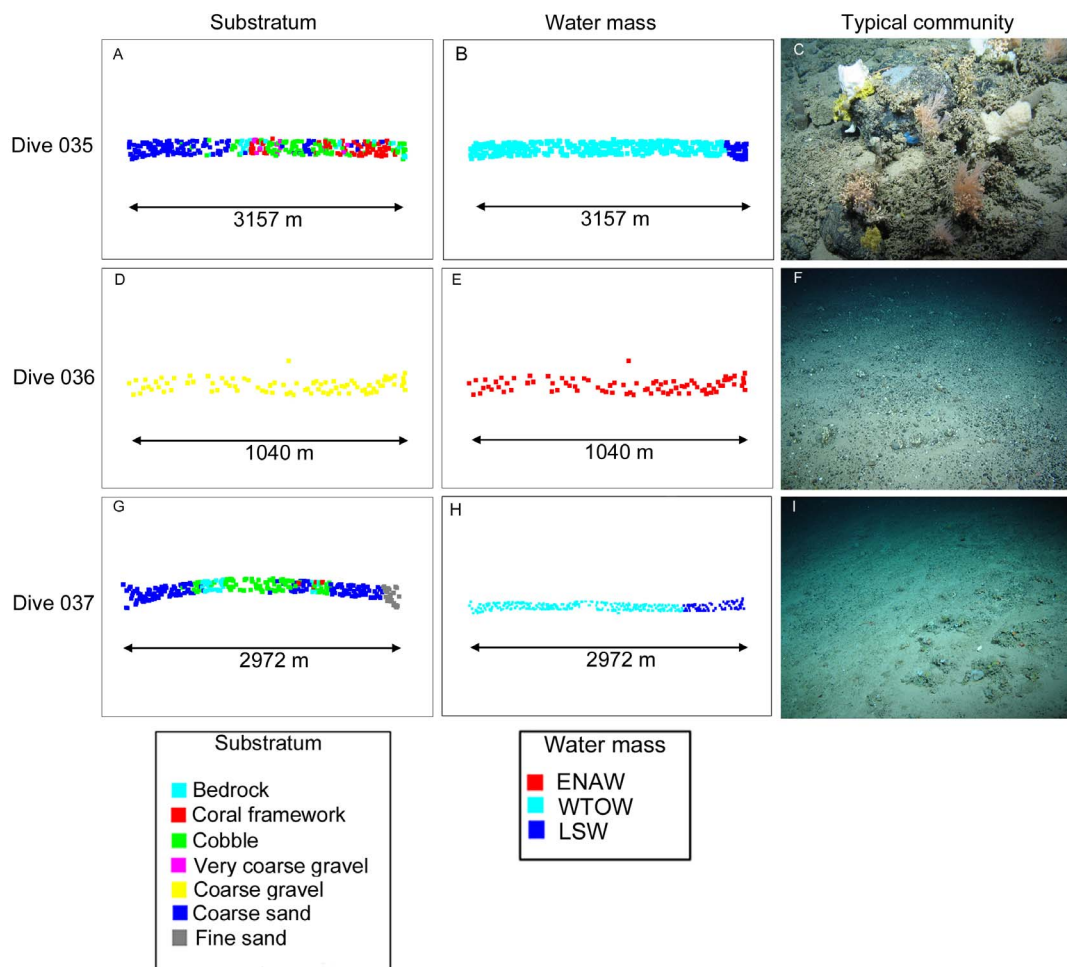


Figure 5 | Spatial gradients in sedimentary facies and water mass structure and the length of each dive transect in a non-metric multidimensional scaling plot. A representative benthic community image is shown in each case using selected ROV images obtained by the authors during the JC073 cruise.

Knowledge of seamount ecology in the wider northeast Atlantic is still poor⁵⁴, but multidisciplinary approaches to collecting these data hold much promise in addressing this gap⁵⁵. Our first investigation of the turnover in the benthic communities and environmental dynamics at the HTS will contribute to the baseline knowledge needed to monitor this and other seamounts in the northeast Atlantic, while subsequent visual surveys should incorporate detailed acoustic data and broader coverage, particularly of the diverse flank habitats.

Methods

ROV seabed surveys. The first visual survey of the HTS was conducted as part of a wider climate change-themed research expedition, the ‘Changing Oceans Expedition’, on the RRS *James Cook* in May–June 2012¹⁵. Three dive transects (Figure 1, Table 1) were conducted using the Irish Marine Institute’s *Holland-I*, a work class Quasar ROV manufactured by Soil Machine Dynamics Ltd. The *Holland-I* was equipped with two manipulator arms, an Insite Mini Zeus video camera with direct HDSDI fibre output, a Kongsberg 14–208 digital stills camera (used for the present study), two 400 Watt Deep-sea Power & Light SeaArc2 HMI lights, two 25,000 lumen Cathx Ocean APHOS LED lights, and two Deep-sea Power & Light lasers 10 cm apart. As there was only time for three ROV transects, dive sites were selected to enable preliminary comparisons between the seamount flanks (dives 035 and 037) summit (dive 036).

CTD profiling and processing. Oceanographic data obtained by CTD were used to help characterise the chemical oceanography of all the different water mass layers at the HTS in order to help explain any differences in species richness or composition across the seamount.

A CTD profile was conducted on the seamount along a full-depth cast at 56°35.295 N and 10°19.65 W. A Sea-Bird 911 plus CTD system (9plus underwater unit and Sea-Bird 11plus deck unit) fitted with a Rosette water sampling unit and

10 L Niskin water bottles was used. Conductivity, temperature and pressure sensors were laboratory calibrated prior to the cruise, giving coefficients for a linear fit. Also attached the Rosette was a Sea-Bird 43 dissolved oxygen sensor, Chelsea Aquatracka MKIII fluorometer (set to detect chlorophyll α : excitation wavelength of 430 nm and emission wavelength of 685 nm), and Chelsea Aquatracka MKIII Transmissometer, to measure dissolved oxygen, chlorophyll fluorescence and a particle attenuation coefficient (C_p) measured at wavelength of 660 nm, respectively, and as described in Findlay *et al.*²³. Data processing was performed using the software SBE Data Processing (V7.21g) and Ocean Data View (V4.3.7) for visualisation. Dissolved oxygen (DO) was calibrated against Winkler titrations made on water samples taken at various depths through the water column as described in Findlay *et al.*²³. The offset between titrations and sensor measurements was <1%.

Borosilicate glass bottles with ground glass stoppers (50 mL) were used to collect seawater from the Niskin bottles for the dissolved inorganic carbon (DIC) and total alkalinity (TA) analysis, at water depths of near surface (2 m), 10, 50, 250, 500, 1000, 1500 and 1930 m. Sample bottles were rinsed, filled and poisoned with 10 μ L mercuric chloride for storage, according to standard procedures detailed in Dickson *et al.*⁵⁶. Duplicate samples were taken from the same Niskin bottle. Samples were brought into the chemical laboratory onboard during the cruise at sea, normalised to room temperature (approximately 24 °C), and analysed for DIC and TA within 24 hours of collection.

A Dissolved Inorganic Carbon Analyser (Apollo SciTech, Model AS-C3) calibrated using CO₂ Certified Reference Materials (Dickson, Batch 113) was used to measure DIC, and duplicate measurements were made to provide an estimate of measurement error, which was 0.2%. DIC was also corrected for the addition of mercuric chloride.

An open-cell potentiometric titration method using an automated titrator (Apollo SciTech Alkalinity Titrator Model AS-ALK2) was used to measure TA, calibrated with CO₂ Certified Reference Materials (Dickson, Batch 113). Duplicate measurements were made for each sample to provide a measurement error, which was 0.4%. TA was also corrected for the addition of mercuric chloride.

TA and DIC, together with depth, temperature and salinity, were used to calculate the remaining carbonate system parameters (pH, pCO₂, Ω aragonite) using the programme CO2sys as described in Findlay *et al.*²³

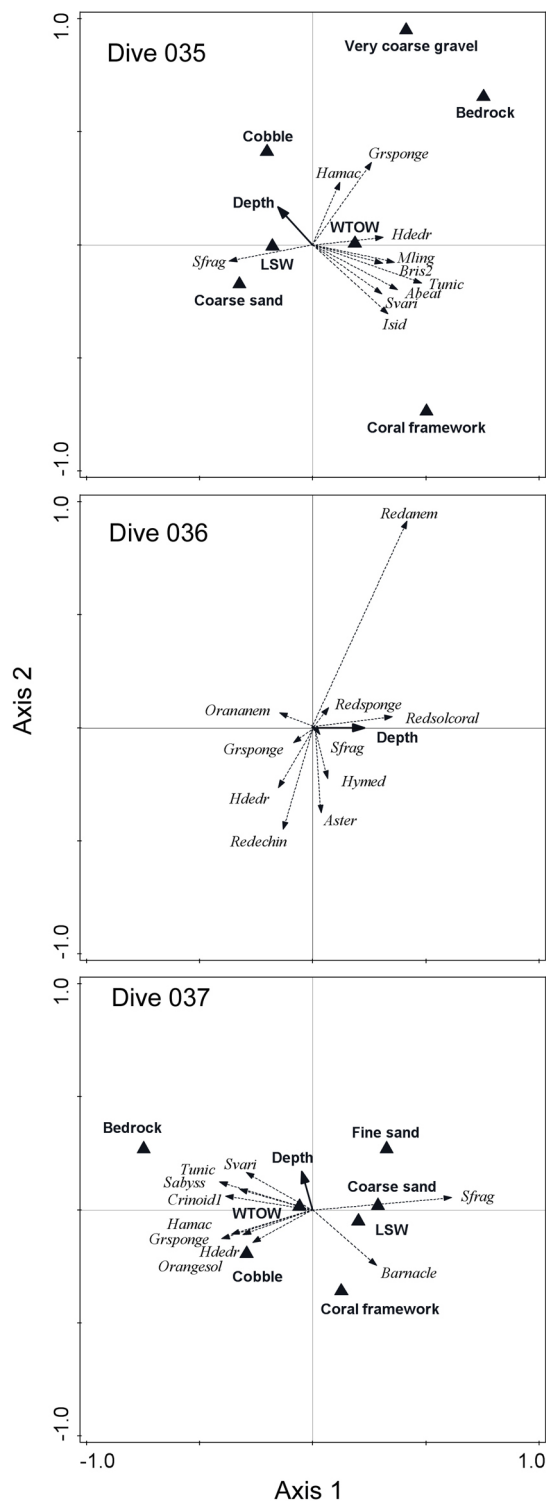


Figure 6 | Species-environment biplots from the flanks (dives 035 and 037) and summit (dive 036) showing the species that were most strongly correlated to the ordination axes. Abbreviations are as follows: Sfrag = *Syringammina fragilissima*; Isid = cf *Isidella* indeterminate species; Svari = *Solenosmia variabilis*; Abeat = *Aprocallistes beatrix*; Tunic = Tunicata; Bris2 = *Brisingiid* sp. 2; Mling = *Mycale lingua*; Hdedr = *Hexadella dedritifera*; Gr.sponge = green encrusting sponge; Hamac = ?*Hamacantha* indeterminate sp.; Redanem = red anemone sp.; Red sponge = red sponge sp.; Redsolcoral = red solitary coral; Orananem = orange anemone sp.; Hymed = *Hymedesmia* cf (*Hymedesmia*) *curvichela*; Aster = asteroid sp. 1; Redechin = red echinoid sp.; Barnacle = barnacle; Orangesol = orange solitary coral; Crinoid1 = crinoid sp. 1; Sabyss = *Stichopathes* cf *abyssicola*.

Best subsets regression analysis using Minitab (v. 16.1.0) showed temperature and salinity to be strong predictors for oxygen saturation state using data from the CTD profile ($r^2 = 99.0$, $r^2_{(adj)} = 99.0$, $Mallows Cp = 48.6$, $S = 0.32238$) according to equation (1):

$$\text{Oxy \%Sat} = (3557 - 100 * \text{Salinity} + 5.83 * \text{Temp}) - 8.1228; \text{ for depth} \geq 1000 \text{ m (1)}$$

Best subset regression analysis of the carbonate system data also revealed that temperature and oxygen saturation (%) were strong predictors for aragonite saturation state ($r^2 = 98.0$, $r^2_{(adj)} = 97.6$, $Mallows Cp = 4.7$, $S = 0.082878$) according to the equation (2):

$$\Omega_{\text{Aragonite}} = -1.54 + 0.0302 * \text{Oxy\%sat} + 0.0877 * \text{Temp} \quad (2)$$

Additional CTD data were collected from a Sea-Bird microCAT CTD attached to the ROV. CTD data processing were performed using the software SBE Data Processing (V7.21g) and Ocean Data View (V4.3.7) for visualisation, and time-matched to the latitudinal and longitudinal positions collected from the ROV log. Equations (1) and (2) were applied to the ROV CTD data to produce estimates for oxygen saturation (%) and $\Omega_{\text{Aragonite}}$.

Image analysis. A subset of ROV still images was created by selecting images taken every 60 seconds during the dive. Blurred images, or those taken at different angles of the same object, were excluded leaving a reduced subset of 697 images. Each image was opened in Picasa viewer v. 3.9 to categorise predominant sedimentary facies and record the presence and absence of megafauna.

For each image, the substratum that was proportionally dominant (>50% of the image) was categorised using a modified Wentworth scale⁵⁷ (Supplementary Table S4). A species matrix was created by enumerating every taxonomically distinct organism in an image as present or absent. Given the high uncertainties of identifying benthos from ROV images without accompanying physical samples, we adopted best practices in habitat analyses⁴⁴ to provide the best possible yet conservative identifications: taxonomic accounts of the fauna in this and adjacent regions were used to distinguish morphologically different species, and the oceanographic setting and associated communities were established to support our preliminary identifications particularly in habitat-forming fauna such as sponges and corals. Finally, our identifications of these and other fauna were verified by senior taxonomic specialists (see Acknowledgements). Indeterminate taxa that could not be confidently distinguished from species already listed in the matrix were excluded from the analyses.

Statistical analyses. Trends in species richness were estimated by multivariate regression to predict the number of square-root-transformed species (richness) at each photographic station using depth, predominant substrata (Supplementary Table S4) and oceanographic layer (dynamic WTOW or stable LSW). Richness was not normally distributed during any ROV dive (Kolmogorov-Smirnov $D_{\text{dive035}} = 0.143$, $p < 0.001$; $D_{\text{dive036}} = 0.151$, $p = 0.039$; $D_{\text{dive037}} = 0.135$, $p < 0.001$); thus, non-parametric locally weighted scatterplot smoothing (LOWESS) regression was conducted for each dive (using XLSTAT v.2008). The standard deviation was used as the bandwidth to smooth the data in a second order polynomial function.

Analysis of similarities (ANOSIM) and similarity of percentages (SIMPER) were used to conduct preliminary analyses of environmental variables that correlated to changes in species composition. Pairwise measures of the Sørensen Index was used to measure community dissimilarity between images, and statistical significance was estimated using ANOSIM between categories of geomorphological feature (summit or flanks), predominant substrata (Supplementary Table S4), and between oceanographic layers (dynamic WTOW or stable LSW layer). Each ANOSIM was based on 999 permutations and yielded an overall global and pairwise values of R that measure the strength of the correlation between the environmental variable and species turnover. SIMPER was conducted for each category to characterise the megafaunal assemblage.

Following this preliminary investigation, we progressed beyond the correlation stage to examine whether environmental variables could explain a statistically significant or large proportion of the species turnover observed during each ROV dive. A canonical variance partitioning statistical approach was used to measure the fraction of species turnover explained specifically by environmental variability, geographic distance between image stations, or induced spatial effects wherein environmental dissimilarity varies with the geographic distance between two images. Redundancy analysis (RDA) was used to constrain species ordinations into linear combinations of explanatory variables, the latter which were then partitioned into the explained by the environment, space, spatially structured environmental gradients, and unconstrained (unexplained) residual inertia. The constrained variance can be further partitioned into the three fractions of pure environmental, spatial and spatially-induced environmental effects by conducting partial canonical analyses (pRDA) as described by Borcard *et al.*⁵⁸. Response variables (species) were Hellinger-transformed presence-absence data⁵⁹. Explanatory variables were depth, the categorical variable oceanographic layer, and the UTM co-ordinates for each image. Variance partitioning was conducted using CANOCO v.5.02⁶⁰.

1. Clark, M. R. *et al.* The ecology of seamounts: structure, function, and human impacts. *Annu. Rev. Mar. Sci.* **2**, 253–278 (2010).



2. Clark, M. R., Schlacher, T. A., Rowden, A. A., Stocks, K. I. & Conslavey, M. Science priorities for seamounts: research links to conservation and management. *PLoS One* **7**, e29232 (2012).
3. Althaus, F. *et al.* Impacts of bottom trawling on deep-coral ecosystems of seamounts are long-lasting. *Mar. Ecol. Prog. Ser.* **397**, 279–294 (2009).
4. McClain, C. R., Lundsten, L., Barry, J. & DeVogelaere, A. Assemblage structure, but not diversity or density, change with depth on a northeast Pacific seamount. *Mar. Ecol.* **31** (Suppl. S1), 14–25 (2010).
5. Williams, A. *et al.* Scales of habitat heterogeneity and megabenthos biodiversity on an extensive Australian continental margin (100–1000 m depths). *Mar. Ecol.* **31**, 222–236 (2010).
6. Baco, A. R. & Cairns, S. D. Comparing molecular variation to morphological species designations in the deep-sea coral *Narella* reveals new insights into seamount coral ranges. *PLoS One* **7**, e45555 (2012).
7. Bett, B. J. UK Atlantic margin environmental survey: introduction and overview of bathyal benthic ecology. *Cont. Shelf Res.* **21**, 917–956 (2001).
8. Kville, K. Ø., Taranto, G. H., Pitcher, T. J. & Morato, T. A global assessment of seamount ecosystems knowledge using an ecosystem evaluation framework. *Biol. Conserv.* **173**, 108–120 (2014).
9. Taranto, G. H., Kville, K. Ø., Pitcher, T. J. & Morato, T. An ecosystem evaluation framework for global seamount conservation and management. *PLoS One* **8**, e42950 (2012).
10. Stewart, H., Davies, J., Long, D., Strömberg, H. & Hitchen, K. JNCC Offshore Natura Survey. Anton Dohrn Seamount and East Rockall Bank areas of search. 2009/03-JNCC Cruise Report, No. CR/09/113 (2009).
11. Howell, K. L., Davies, J. S. & Narayanaswamy, B. E. Identifying deep-sea megafaunal epibenthic assemblages for use in habitat mapping and marine protected area network design. *J. Mar. Biol. Assoc. U.K.* **90**, 33–68 (2010).
12. Howell, K. L., Mowles, S. L. & Foggo, A. Mounting evidence: near-slope seamounts are faunally indistinct from an adjacent bank. *Mar. Ecol.* **31** (Suppl. 1), 52–62 (2010).
13. Bullimore, R., Foster, N. & Howell, K. Coral-characterized benthic assemblages of the deep Northeast Atlantic: defining “Coral Gardens” to support future habitat mapping efforts. *ICES J. Mar. Sci.* **70**, 511–522 (2013).
14. Long, D., Howell, K. L., Davies, J. & Stewart, H. JNCC Offshore Natura survey of Anton Dohrn Seamount and East Rockall Bank Areas of Search. *JNCC Report Series* 437 (2010).
15. Roberts, J. M. and shipboard party. Changing Oceans Expedition 2013. RRS *James Cook* 073 Cruise Report (2013).
16. O’Connor, J. M., Stoffers, P., Wijbrans, J. R., Shannon, P. M. & Morrissey, T. Evidence from episodic seamount volcanism for pulsing of the Iceland plume in the last 70 Myr. *Nature* **408**, 954–958 (2000).
17. Long, D. & Holmes, R. Submarine landslides and tsunami threat to Scotland. Paper presented at The Proceedings of the International Tsunami Symposium (ITS), Seattle: University of Washington. 2001, August 7–9. pp. 355–366 (2001).
18. Sacchetti, F. *et al.* Deep-water geomorphology of the glaciated Irish margin from high-resolution marine geophysical data. *Mar. Geol.* **291–294**, 113–131 (2012).
19. Jacobs, C. L. An appraisal of the surface geology and sedimentary processes within SEA7, the UK continental shelf. National Oceanography Centre, Southampton (2006). *Research and Consultancy Report*, 18 (2006).
20. Boisseau, O., Moscrop, A., Cucknell, A., McLanaghan, R. & Wall, D. An acoustic survey for beaked whales in the Rockall Trough. Report to the International Whaling Commission, SC/63/SM.2, 1–12 (2011).
21. ICES. Report of the Working Group on the Biology and Assessment of Deep-Sea Fisheries Resources (WGDEEP), 8–15 May 2007, ICES Headquarters. ICES CM 2007/ACFM. 20(2007).
22. ICES. *International Council for the Exploration of the Sea Advice 2010*, Book 9, Section 9.4.14, pp. 211–216 (2010).
23. Findlay, H. S. *et al.* Fine-scale nutrient and carbonate system dynamics around cold-water coral reefs in the northeast Atlantic. *Sci. Rep.* **4**, 3671 (2014).
24. Gordon, J. D. M. Deep-water fisheries at the Atlantic Frontier. *Cont. Shelf Res.* **21**, 987–1003 (2001).
25. McGrath, T., Kivimäe, C., Tanhua, T., Cave, R. R. & McGovern, E. Inorganic carbon and pH levels in the Rockall Trough 1991–2010. *Deep Sea Res. I* **68**, 79–91 (2012).
26. McGrath, T., Nolan, G. & McGovern, E. Chemical characteristics of water masses in the Rockall Trough. *Deep Sea Res. I* **61**, 57–73 (2012).
27. Gage, J. D., Lamont, P. A., Kroeger, K., Paterson, G. L. J. & Gonzalez Vecino, J. L. Patterns in deep-sea macrobenthos at the continental margin: standing crop, diversity and faunal change on the continental slope of Scotland. *Hydrobiologia* **440**, 261–271 (2000).
28. Johnson, C., Sherwin, T., Smythe-Wright, D., Shimmiel, T. & Turrell, W. R. Wyville Thomson Ridge Overflow Water: spatial and temporal distribution in the Rockall Trough. *Deep Sea Res. I* **57**, 1153–1162 (2010).
29. New, A. L. & Smythe-Wright, D. Aspects of the circulation in the Rockall Trough. *Cont. Shelf Res.* **21**, 777–810 (2001).
30. Henry, L.-A., Moreno Navas, J., Hennige, S. J., Wicks, L. C., Vad, J. & Roberts, J. M. Cold-water coral reef habitats benefit recreationally valuable sharks. *Biol. Conserv.* **161**, 67–70 (2013).
31. Konráðsdóttir, S. Úrhlutun og þáttun efna úr svömpunum *Petrosia crassa* og *Halichondria sitchensis* og skimun fyrir krabbameinsfrumuhemjandi áhrifum þeirra in vitro. Unpublished thesis, University of Iceland. <http://hdl.handle.net/1946/11191> (2012).
32. Moore, J. A. *et al.* False boarfish *Neocyttus helgae* in the western North Atlantic. *Bull. Peabody Mus. Nat. Hist.* **49**, 31–41 (2008).
33. Cárdenas, P. *et al.* Taxonomy, biogeography and DNA barcodes of *Geodia* species (Porifera, Demospongiae, Tetractinellida) in the Atlantic boreo-arctic region. *Zool. J. Linn. Soc.* **169**, 251–311 (2013).
34. Roberts, J. M., Henry, L.-A., Long, D. & Hartley, J. P. Cold-water coral reef frameworks, megafaunal communities and evidence for coral carbonate mounds on the Hatton Bank, north east Atlantic. *Facies* **54**, 297–316 (2008).
35. Durán Muñoz, P. *et al.* Effects of deep-sea bottom longlining on the Hatton Bank fish communities and benthic ecosystem, north-east Atlantic. *J. Mar. Biol. Assoc. U.K.* **91**, 939–952 (2011).
36. Narayanaswamy, B. E., Hughes, D. J., Howell, K. L., Davies, J. & Jacobs, C. First observations of megafaunal communities inhabiting George Bligh Bank, Northeast Atlantic. *Deep Sea Res. II* **92**, 79–86 (2013).
37. Long, D. J. & Baco, A. R. Rapid change with depth in megabenthic structure-forming communities of the Makapu’u deep-sea coral bed. *Deep Sea Res. II* **99**, 158–168 (2014).
38. Mohn, C., White, M., Bashmachnikov, F. J. & Pelegrí, J. L. Dynamics at an elongated, intermediate depth seamount in the North Atlantic (Sedlo Seamount, 40°20’N, 26°40’W). *Deep Sea Res. I* **56**, 2582–2592 (2009).
39. Morris, K. J., Tyler, P. A., Masson, D. G., Huvette, V. A. I. & Rogers, A. D. Distribution of cold-water corals in the Whittard Canyon, NE Atlantic Ocean. *Deep Sea Res. II* **92**, 136–144 (2013).
40. Piepenburg, D. & Müller, B. Distribution of epibenthic communities on the Great Meteor Seamount (North-east Atlantic) mirrors pelagic processes. *Arch. Fish. Mar. Res.* **51**, 55–70 (2004).
41. Xing, J. & Davies, A. M. A three-dimensional model of internal tides on the Malin-Hebrides shelf and shelf edge. *J. Geophys. Res.* **103**, 27821–27847 (1998).
42. Stashchuk, N. & Vlasenko, V. Topographic generation of internal waves by nonlinear superposition of tidal harmonics. *Deep Sea Res. I* **52**, 605–620 (2005).
43. Hall, P. & Davies, A. M. Comparison of finite difference and element models of internal tides on the Malin-Hebrides Shelf. *Ocean Dynam.* **55**, 272–293 (2005).
44. Henry, L.-A. & Roberts, J. M. Recommendations for best practice in deep-sea habitat classification – Bullimore *et al.* as a case study. *ICES J. Mar. Sci.* **71**, 895–898 (2014).
45. Lundsten, L. *et al.* Benthic invertebrate communities on three seamounts off southern and central California, USA. *Mar. Ecol. Prog. Ser.* **374**, 23–32 (2009).
46. Davies, A. J. & Guinotte, J. M. Global habitat suitability for framework-forming cold-water corals. *PLoS One* **6**, e18483 (2011).
47. Flögel, S., Dullo, W.-C., Pfannkuche, K., Kiriakoulakis, K. & Rüggeberg, A. Geochemical and physical constraints for the occurrence of living cold-water corals. *Deep Sea Res. II* **99**, 19–26 (2014).
48. Tracey, D. M., Rowden, A. A., Mackay, K. A. & Compton, T. Habitat-forming cold-water corals show affinity for seamounts in the New Zealand region. *Mar. Ecol. Prog. Ser.* **430**, 1–22 (2011).
49. Roberts, J. M., Harvey, S. M., Lamont, P. A., Gage, J. D. & Humphery, J. D. Seabed photography, environmental assessment and evidence for deep-water trawling on the continental margin west of the Hebrides. *Hydrobiologia* **441**, 173–183 (2000).
50. Henry, L.-A. & Roberts, J. M. Biodiversity and ecological composition of macrobenthos on cold-water coral mounds and adjacent off-mound habitat in the bathyal Porcupine Seabight, NE Atlantic. *Deep Sea Res. I* **54**, 654–672 (2007).
51. Benn, A. R. *et al.* Human activities on the deep seafloor in the North East Atlantic: an assessment of spatial extent. *PLoS One* **5**, e12730 (2010).
52. Lorange, P. Structure du peuplement ichthyologique du talus continental à l’ouest des Iles Britanniques et impact de la pêche. *Cybiurn* **22**, 309–331 (1998).
53. Haedrich, R. L., Merrett, N. R. & O’Dea, N. R. Can ecological knowledge catch up with deep-water fishing? a North Atlantic perspective. *Fish. Res.* **51**, 113–122 (2001).
54. Morato, T. *et al.* Seamount physiography and biology in the north-east Atlantic and Mediterranean Sea. *Biogeosciences* **10**, 3039–3054 (2013).
55. Wienberg, C., Wintersteller, P., Beuck, L. & Hebbeln, D. Coral Patch seamount (NE Atlantic) – a sedimentological and megafaunal reconnaissance based on video and hydroacoustic surveys. *Biogeosciences* **10**, 3421–3443 (2013).
56. Dickson, A. G., Sabine, C. L. & Christian, J. R. Guide to best practices for ocean CO₂ measurements. *PICES Spec. Publ.* **3**, IOCCP report No. 8 (2007).
57. Wentworth, C. K. A scale of grade and class terms for clastic sediments. *J. Geol.* **30**, 377–392 (1922).
58. Borcard, D., Legendre, P. & Drapeau, P. Partialling out the spatial component of ecological variation. *Ecology* **73**, 1045–1055 (1992).
59. Legendre, P. D. & Gallagher, E. D. Ecologically meaningful transformations for ordination of species data. *Oecologia* **129**, 271–280 (2001).
60. Ter Braak, C. J. F. & Šmilauer, P. *Canoco Reference Manual and User’s Guide, Software for Ordination (Version 5)*. (Biometris, Wageningen and České Budějovice, 2012).

Acknowledgments

The Science Party acknowledge the significant efforts of Bill Richardson (Master) and the entire crew of the RRS *James Cook*. Further thanks are due Will Handley and the *Holland-I*



ROV team. The authors are grateful to the following experts for providing critical taxonomic expertise: Stephen Cairns (Scleractinia), Louise Allcock (Octopoda), Tina Molodtsova (Antipatharia), Alvaro Altuna (Alcynoacea), Roger Bamber (Pycnogonida), Rob van Soest, Paco Cárdenas and Martin Dohrmann (all Porifera). The JC073 cruise was funded through the Natural Environment Research Council (NERC) UK Ocean Acidification (UKOA) research programme's Benthic Consortium project (NE/H017305/1). JMR acknowledges support from Heriot-Watt University's Environment and Climate Change theme. Supplementary shiptime funding for the ROV seamount surveys was received from the Joint Nature Conservation Committee with the agreement of NERC. We thank Marina Cunha for providing comments.

Author contributions

L.-A.H. and H.S.F. wrote the main manuscript text and prepared figures 4–6 and all tables. L.-A.H. contributed the statistical analyses and consulted with taxonomic experts for species verification. J.V. conducted the image annotations. H.S.F. analysed the carbonate chemistry on the seamount and prepared figures 2 and 3. J.M. and R.M. contributed text on coral, sponge and fish diversity and biogeography. J.M.R. was chief scientist and principal investigator on the “Changing Oceans Expedition” research cruise and prepared Figure 1. All authors reviewed the manuscript.

Additional information

Supplementary information accompanies this paper at <http://www.nature.com/scientificreports>

Competing financial interests: The authors declare no competing financial interests.

How to cite this article: Henry, L.-A. *et al.* Environmental variability and biodiversity of megabenthos on the Hebrides Terrace Seamount (Northeast Atlantic). *Sci. Rep.* **4**, 5589; DOI:10.1038/srep05589 (2014).



This work is licensed under a Creative Commons Attribution-NonCommercial-NoDerivs 4.0 International License. The images or other third party material in this article are included in the article's Creative Commons license, unless indicated otherwise in the credit line; if the material is not included under the Creative Commons license, users will need to obtain permission from the license holder in order to reproduce the material. To view a copy of this license, visit <http://creativecommons.org/licenses/by-nc-nd/4.0/>